Journal of Thermal Analysis and Calorimetry, Vol. 94 (2008) 2, 545–551

RIGID AMORPHOUS FRACTION IN POLY(ETHYLENE TEREPHTHALATE) DETERMINED BY DILATOMETRY

P. Slobodian[*]

Tomas Bata University in Zlín, Faculty of Technology, T.G.M. 275, 762 72 Zlín, Czech Republic

Volumetric thermal analysis of semicrystalline poly(ethylene terephthalate), PET, with different content of crystalline phase was carried out using mercury-in-glass dilatometry. The effect of crystals on the thermal properties of amorphous phase (glass transition temperature, T_g, thermal expansion coefficients, α) were determined. At cold-crystallization (106°C, up to 4 h), crystalline content of 2.4–25.3 vol.% was achieved. Increasing content of crystalline phase broadens the glass transition region and increases T_g. The change of thermal expansion coefficient during glass transition is lower than that predicted by the two-phase model, which indicates the presence of a third fraction – rigid amorphous fraction (RAF), whose content steadily increases during crystallization. However, its relative portion (specific RAF) is significantly reduced. Further significant decrease in specific RAF appears after annealing at a higher temperature.

Keywords: *cold-crystallization, dilatometry, glass transition temperature, poly(ethylene terephthalate), rigid amorphous fraction*

Introduction

Semicrystalline poly(ethylene terephthalate), PET, generally consists of two phases with different structures and properties. One of them is the crystalline phase, where molecules are arranged into lamellae further associated into larger objects, e.g. spherulites, and the other is the amorphous phase represented by disordered molecules or their parts situated in both inter-spherulitic and intra-spherulitic amorphous regions. However, the existence of a third fraction, often denoted as a rigid amorphous fraction of the amorphous phase, RAF, can be revealed experimentally. Thus, the sample can be considered to consist of three fractions: crystalline, RAF and MAF (mobile amorphous fraction) [1-17]. Nevertheless, this is not only the case of PET but also other semicrystalline polymers show the existence RAF, such as PTFE [18], PA-6 [9, 19], PC [20], poly(phenylene sulfide) [21] or poly(*L*-lactic acid) [22].

Experimental techniques, such as differential scanning calorimetry, DSC, or temperature-modulated DSC, are usually capable of quantifying this fraction as a deficiency in the difference in heat capacity, Δc_p, at glass transition temperature, T_g [1–9], or from enthalpy relaxation experiments performed in the glass transition region [8, 10–13]. However, the character of the amorphous phase in semicrystalline PET can be also investigated by other methods like dynamic mechanical analyses, DMA [12, 14, 15], which also reveals the existence of a third fraction, dielectric spectroscopy [13, 16] or positron annihilation life time spectroscopy [17].

RAF arises from the strain at the crystal-amorphous interphase produced by polymer molecules incorporated into both regions. The strain constrains the local segmental mobility of amorphous parts of molecules, which significantly modifies their properties due to the layer of disordered but hindered molecules or their parts which is created on the surface of crystals. The analysis of PET revealed that the thickness of RAF at the surface of lamellae is about 2–4 nm, and is almost independent of the lamella thickness [3, 5, 17]. It is widely accepted that the formation of RAF is coupled with the formation of crystals and their devitrification with melting or continuously between the glass transition temperature, T_g, and crystallization temperature, T_c [3–5, 17, 23]. Such conclusions were made according to precision studies, e.g. the studies focused on oxygen transport/solubility [5] or results obtained from positron annihilation lifetime spectroscopy [17]. It was reported that the specific volume of RAF increases with an increase of T_c [5], or that fractional free volume is related to that of the equilibrium melt at T_c [17], both concluding that RAF becomes vitrified at the crystallization temperature.

From the macroscopic point of view, semicrystalline PET incorporates two different amorphous regions with different thermal properties [1–12], relaxation kinetics [8, 10–13, 23, 24] or macroscopic mechanical behaviour [7, 14, 24, 25]. The effect of RAF is obvious in changes of thermal properties of

* Slobodian@ft.utb.cz

1388–6150/$20.00

Akadémiai Kiadó, Budapest, Hungary
Springer, Dordrecht, The Netherlands

the amorphous phase, like broadening of the glass transition region together with shifting of conventionally evaluated T_g, representing just one temperature point of extensive transition region, to higher temperatures. The observed changes in specific heat, c_p, or thermal expansion coefficient, α, associated with glass transition as Δc_p or $\Delta\alpha$ depending on the content of crystallinity, are found to be inconsistent with the two-phase model. Based on these facts, some material is expected to be in the form of RAF.

Overall, semicrystalline PET can be prepared in a wide range of crystallinity as a result of the thermal treatment in the temperature region between the glass transition temperature, T_g, and melting temperature, T_m, and at both principal regimes, i.e. the cold-crystallization or the melt-crystallization (classified from the direction in which crystallization temperature is approached). The effect of crystals onto amorphous regions depends not only on the degree of crystallinity but also on the structure of the crystalline phase, like the size and distribution of lamellae, and hence crystallization conditions, i.e. crystallization temperature or cold- *vs.* melt-crystallization [5, 13]. Cold-crystallization results in the formation of imperfect crystals showing a relatively large amount of RAF, while melt-crystallized PET contains a larger number of lamellar stacks in the crystalline fraction. The fraction of RAF was found to increase steadily with crystallinity and seems to level off at the final stage of cold-crystallization [3]. However, the ratio of RAF to the crystalline fraction, specific RAF, decreases during cold-crystallization or at subsequent annealing. Calorimetric and X-ray analyses indicate changes of the crystal morphology and increasing perfection of the crystals, which results in a decrease of local strain at the crystal surface and of the amount of specific RAF.

Although poly(ethylene terephthalate) is a material of common use and suitable calorimetric thermal data is generally known, volumetric analyses providing appropriate data are very sporadic. However, the presence of RAF and its actual content plays a significant role in effective use of PET in practice, e.g. recycling of PET packaging materials.

In this paper, volumetric thermal analysis of semicrystalline PET in a broad range of crystallinity from nearly amorphous material (2.4 vol.% – prepared by quenching of PET melt into room-temperature water) to pseudo-equilibrium PET (25.3 vol.% – crystallized at 106°C by cold-crystallization) was carried out. The effect of crystalline content onto the volumetric glass transition temperature and thermal expansion coefficients was determined. The presence of the rigid amorphous fraction was detected and its amount quantified.

Experimental

PET was purchased from Aldrich Chemical Company. From the original granules the specimen for dilatometric measurements was prepared by pouring the melted polymer (290°C) into room-temperature water.

A mercury-in-glass dilatometer was prepared according to ASTM Standard D 864-52 [26]. The dilatometer with the specimen was filled with pure mercury (99.999%) under vacuum of about 2 Pa. Thermal programs were followed by immersing the dilatometer into precision programmable thermostatic bath Julabo HP 4 with a thermal stability of ±0.02°C. Volume-temperature dependences were measured during uniform cooling at 1°C min^{-1} from the initial temperature T_i=90°C, where the sample was heated for 15 min, to 48°C (in order to erase any previous thermal history of the specimen prior to cooling). The lag between the temperature of silicon oil bath and the temperature inside the dilatometer was measured to be 0.7°C. It was determined with a K-type thermocouple placed inside the sample inserted into a dilatometer with the same geometry and amount of sample and mercury as in the testing dilatometer. All experimental data was corrected by this value.

Different levels of crystallinity were reached by the varying way of crystallization. Cold-crystallization was done at 106°C by immersing the dilatometer into the precision thermostatic bath; the times were from 10 up to 256 min, and additional long-term annealing at the same temperature was performed for 74 h (4440 min). Finally, annealing at 245°C for 60 min was performed. Then the dilatometer was refilled with mercury to scan the volume-temperature dependence. Crystallinity was determined by density measurements after breaking up the dilatometer.

Results and discussion

The density of the prepared quenched PET sample inserted into the dilatometer was measured to be ρ=1.3391 g cm^{-3}. Compared to the density of pure amorphous PET, ρ_a=1.335 g cm^{-3} [27] and to the calculated density of crystalline phase, ρ_c=1.515 g cm^{-3} [28], the degree of crystallinity can be expressed as the mass fraction, w, or volume fraction, φ, Eqs (1) and (2), both under the assumption of additivity of amorphous and crystalline phases:

$$\varphi_c = \frac{\rho - \rho_a}{\rho_c - \rho_a} \quad (1)$$

$$w_c = \frac{\rho_c(\rho - \rho_a)}{\rho(\rho_c - \rho_a)} \quad (2)$$

The calculated values were w=2.6 mass% and φ=2.3 vol.%. Moreover, an independent determination of the sample crystallinity was carried out using a wide-angle X-ray diffraction (HZG 4 Diffractometer) giving the degree of crystallinity 2.1% [8], which is in a good agreement with volumetric measurements.

The temperature dependence of the difference in specific volume is presented in Fig. 1. It was measured during uniform cooling from equilibrium above T_g to glassy state here presented as examples for the original PET sample (φ=2.3 vol.%) and for other four selected crystallinities, covering the crystallization range. The values of Δν were only used to make data graphically comparable for different crystallinities, and were calculated as $\Delta\nu=\nu_{(T)}-\nu_{(48.5°C)}$. The temperature scan of the original sample clearly demonstrates the method of determination of T_g and thermal expansions coefficients, α. In this concept, the glass transition temperature is determined as the intersection of the equilibrium liquid and asymptotic glassy trails, represented in Fig. 1 by full lines. This corresponds to T_g=68.5±0.3°C.

The standard deviation was calculated from a set of cooling experiments and this value was also used as a typical value for the other specimens. Thermal expansion coefficients above and below T_g (α_l and α_g, respectively) were calculated as the slopes of these lines, as given by Eq. (3) [26].

$$\alpha = \frac{1}{\nu}\frac{\mathrm{d}\nu}{\mathrm{d}T} \tag{3}$$

Overall, it seems to be problematic to measure α_l because of possible concurrent processes with thermal expansion and crystallization or re-crystallization occurring between T_g and T_m. Practically, α_l could be measured in a relatively narrow temperature range, slightly above T_g but below the cold-crystallization temperature range. In the present study, the maximum temperature of cooling experiments was selected to be 90°C; no cold-crystallization prior to cooling was observed. The values of thermal expansion coefficients for the initial PET were $\alpha_l=(5.55\pm0.07)\cdot10^{-4}$ K^{-1} and $\alpha_g=(2.31\pm0.03)\cdot10^{-4}$ K^{-1}, leading to $\Delta\alpha=\alpha_l-\alpha_g=(3.24\pm0.10)\cdot10^{-4}$ K^{-1}. This is actually a jump in α at glass transformation, representing the transformation of mobile amorphous fraction, MAF, which is bulk amorphous PET. The standard deviations were calculated using the Student t distribution, probability of er-

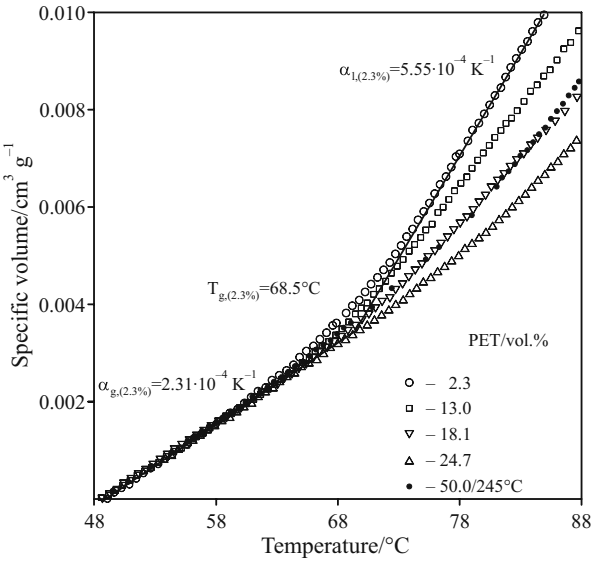

Fig. 1 Difference in specific volume–temperature dependence during uniform cooling by 1°C min^{-1} from equilibrium above glass transition temperature, T_g, to glassy state for PET with crystalline content indicated; T_g and thermal expansion coefficient, α, evaluation

Table 1 Data for different crystallization times, t, for cold-crystallized PET at 106°C, and final 60 min exposure at 245°C. φ_c represents volume fraction of crystalline phase, T_g glass transition temperature, α thermal expansion coefficients (α_l for the liquid state, α_g for the glassy state), $\Delta\alpha=\alpha_l-\alpha_g$, volume fractions of RAF and MAF as φ_{RAF} and φ_{MAF}, respectively, and φ_{RAF}/φ_c means specific RAF

t/min	φ_c/%	T_g/°C	$\alpha_l/10^4$ K^{-1}	$\alpha_g/10^4$ K^{-1}	$\Delta\alpha/10^4$ K^{-1}	φ_{RAF}/%	φ_{MAF}/%	φ_{RAF}/φ_c
–	2.3±0.4	68.5±0.3	5.55±0.07	2.31±0.03	3.24±0.10	12.2	85.5	5.4
10	3.8±0.6	68.3±0.3	5.20±0.08	2.25±0.04	2.95±0.12	18.4	77.8	4.9
18	6.4±0.6	68.0±0.3	4.82±0.06	2.22±0.04	2.60±0.10	25.0	68.6	3.9
26	10.2±0.7	69.0±0.3	4.53±0.06	2.24±0.05	2.29±0.11	29.4	60.4	2.9
32	13.0±0.7	69.3±0.3	4.20±0.07	2.25±0.06	1.95±0.13	35.5	51.5	2.7
40	18.1±0.7	71.2±0.3	3.80±0.05	2.29±0.03	1.51±0.08	42.0	39.8	2.3
48	20.9±0.8	73.9±0.3	3.60±0.07	2.32±0.04	1.28±0.11	45.3	33.8	2.2
56	22.8±0.8	74.3±0.3	3.58±0.06	2.33±0.04	1.25±0.10	44.2	33.0	1.9
86	24.7±0.8	77.9±0.3	3.53±0.05	2.33±0.04	1.17±0.09	44.5	30.9	1.8
126	25.2±0.8	79.7±0.3	3.62±0.08	2.44±0.04	1.18±0.12	43.7	31.1	1.7
246	25.3±0.8	79.6±0.3	3.60±0.08	2.43±0.03	1.17±0.11	43.8	30.9	1.7
4440	28.5±0.8	79.1±0.3	3.63±0.08	2.54±0.03	1.09±0.11	42.7	28.8	1.5
60/245°C	50.0±1.0	74.9±0.3	4.35±0.07	2.61±0.04	1.74±0.11	4.1	45.9	0.1

ror 0.005, and are presented in Table 1 (and further as error bars in Fig. 3).

Figure 1 also demonstrates changes in the character of temperature scans with crystallinity. Although below T_g the slopes seem to be nearly identical, the effect of crystals on thermal properties appears significantly above T_g. Here α_l decreases with crystallinity. Another interesting phenomenon is the shift of the glass transition region to higher temperatures and its broadening. On the contrary, the data for highly crystallized PET achieved after annealing at 245°C shows partial return to higher values of α_l, the glass transition shifts to lower temperatures and the T_g region seems to be narrower.

For the determination of the crystallization process it was necessary to find a temperature which would enable safe manipulation with the dilatometer, in other words, to get different crystallinities with only one dilatometer. The optimum temperature was found to be T_c=106°C. The isothermal crystallization data as a dependence of $X_{(t_c)}$ on logarithm of crystallization time, t_c, at this temperature is presented in Fig. 2. Symbol $X_{(t_c)}$ represents the level of crystallization according to Eq. (4), where ν_0 means initial specific volume, ν_∞ is equilibrium specific volume, and $\nu_{(t_c)}$ stands for specific volume at time t_c.

$$X_{(t_c)} = \frac{\nu_0 - \nu_{(t_c)}}{\nu_0 - \nu_\infty} \quad (4)$$

The crystallization times, t_c, and corresponding values of volume fraction of crystallinity, φ, are given in Table 1. The standard deviations of φ_c presented in the table were calculated from the volume reading accuracy of the mercury-in-glass dilatometer determined according to the dilatometer parameters and thermal fluctuation of the used thermostatic bath, which was $3\cdot10^{-5}$ cm^3 cm^{-3}. The crystallization isotherm given in Fig. 2 represents a typical sigmoid curve with an initial plateau, then it goes through an inflection point (beginning of crystallization) and finally approaches a pseudo-equilibrium value, which is around 25.3 vol.% crystallinity (after approximately 4 h at T_c).

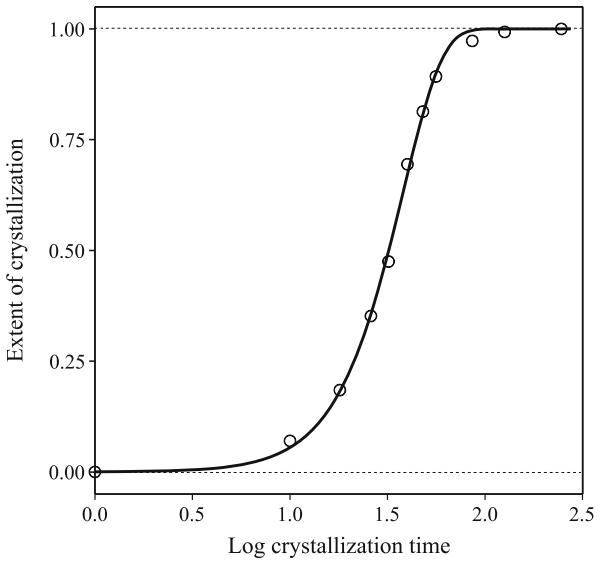

Fig. 2 Volume crystallization isotherm of PET at cold-crystallization temperature 106°C. The full line represents the best fit by Avrami equation, Eq. (5)

The crystallization isotherm was analyzed assuming that the extent of crystallization, $X_{(t_c)}$, with time could be described by the Avrami equation, Eq. (5).

$$1-X_{(t_c)} = \exp\left|-Z(t_c)^n\right| \quad (5)$$

where Z is a rate constant, and n represents a constant of crystallization mechanism. The calculated values of the constants were log$Z$=–3.40±0.23 and n=2.15±0.15. The function is represented by the full line in Fig. 2 and was obtained as a least square fit of Eq. (4). Half-time of crystallization, $\tau_{1/2}$, defined as the middle of crystallization completion, was determined to be 32 min. The calculated values of Avrami constants were found to be in good agreement with data published in [13], log$Z$=–3.65, n=2.30 and $\tau_{1/2}$=33 min measured by DSC, crystallized also at 106°C and for the same type of initial PET (before cold-crystallization). In the mentioned reference the initial PET sample was prepared by pouring melted PET into icy water. The authors report a residual degree of crystallinity not statistically different from zero. In such quenched samples the existence of mesomorphic domains can be supposed, which can be proved, for example, by a lower heat capacity increment in T_g [4]. Finally, such domains are considered to be precursors for a subsequent crystallization process affecting its kinetics. This should be a reason why another study [29] presents slightly different characteristics for PET crystallized at T_c=105°C: log$Z$=–3.17, n=1.7 and $\tau_{1/2}$=59 min. Here, the material was pure amorphous PET as delivered by the supplier.

The values of pseudo-equilibrium crystallinity around 25% can be considered typical of cold-crystallized PET at adequate crystallization temperatures [3, 5, 30]. Slight discrepancies in literature data, between 24–27%, can be partly attributed to the differences in densities of pure amorphous and crystallized PET which are used for crystallinity calculations according to Eqs (1) and (2). For example, a relatively broad range is reported for ρ_c=1.420–1.515 g cm^{-3} [27]. Some inconsistencies can also be found with varying crystallization temperature. Increasing T_c leads to an increase in crystallinity, for example in the range of T_c=95–185°C crystallinities between 24 and 34% were determined [30].

The data in the table shows further increase in crystallinity to some 28.5 vol.% after next long-term crystallization at 106°C (74 h). Finally, when the tem-

perature of annealing is increased to 245°C, a temperature close to melting of crystals, the sample is highly crystallized, with the density ρ=1.4250 g cm^{-3} and the content of crystalline phase 50.0 vol.%.

The research also followed the dependences of specific volume on temperature at the cooling rate of 1°C min^{-1} for each crystalline content, and the values of T_g, α_l, α_g and $\Delta\alpha$ were calculated by the same methods as described above; they are presented in Fig. 3 and summarized again in Table 1. As could be expected, T_g tends to increase with the degree of crystallization, but the rise is not linear. At the beginning, actually, a slight decrease could be observed, then, up to some 13.0 vol.%, it increases gradually, and in the second half of the graph, the increase is quite steep. For φ=25.3 vol.% at a pseudo-equilibrium state after 246 min, T_g achieves 79.6°C. After further annealing at 106°C the value remains more or less constant, within the range of experimental accuracy, but for highly crystallized PET it clearly decreases to some 74.9°C. This can be explained by the decrease in RAF content.

It is usually reported that the glass transition temperature of PET in its amorphous and semicrystalline forms differs by some 10°C. When studied by various experimental methods and under various conditions the values of T_g were found 67–76°C for amorphous and 81–86°C for highly crystalline PET [8, 10, 27, 30]. The crystallinity dependence of T_g measured by DSC and dynamic mechanical analyses (DMA) is presented in [30]. For PET crystallized at 130°C the authors found comparable values of T_g for both experimental methods with the same dependence on crystallinity content as in the present paper, Fig. 3. Here T_g increases non-linearly

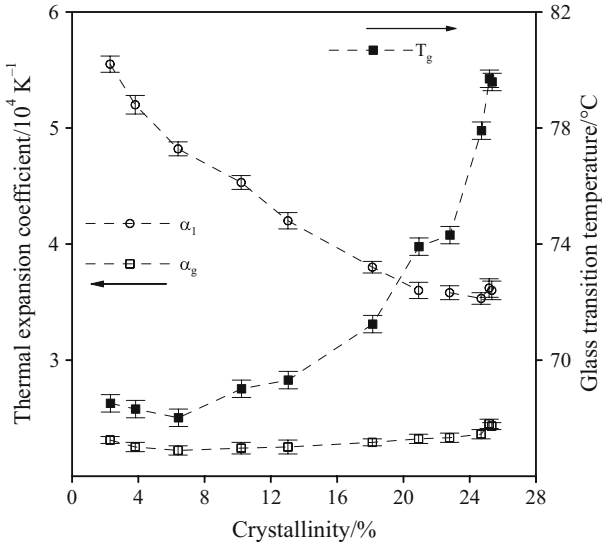

Fig. 3 Dependences of glass transition temperature, T_g and thermal expansion coefficients above, and below $T_g\alpha_l$ and α_g, respectively on volume content of crystalline fraction for cold-crystallized PET at 106°C

with crystallinity, with a sharp rise as it approaches pseudo-equilibrium. On the other hand, literature more often presents a linear dependence. For example, results determined by DMA [14] for PET crystallized at T_c=130°C contain only linear E' and tanδ dependences, or dielectric thermal analysis [13] shows T_g linearly increasing with crystallinity for T_c=140°C.

Figure 3 also shows the changes in the thermal expansion coefficient, α_l, with crystallinity. As can be seen, it decreases from the value of $5.55\cdot10^{-4}$ to $3.60\cdot10^{-4}$ K^{-1}, and seems to reach asymptotically $\alpha_l=3.6\cdot10^{-4}$ K^{-1} at pseudo-equilibrium. Neither here the decrease is linear. From the first three lowest crystallinities the value for pure amorphous PET was extrapolated to be $\alpha_{l,a}=6.25\cdot10^{-4}$ K^{-1}. On the contrary, the thermal expansion coefficient for the glassy state, α_g, is largely independent of the crystalline content, with values ranging between $2.22\cdot10^{-4}$ and $2.44\cdot10^{-4}$ K^{-1}. The value for pure amorphous PET was extrapolated and determined to be $\alpha_{g,a}=2.46\cdot10^{-4}$ K^{-1}; thus, considering $\alpha_{l,a}$ given above, $\Delta\alpha_a=3.79\cdot10^{-4}$ K^{-1}. The values for highly crystallized PET yield a significant increase in α_l at 25.3 vol.% and only a slight increase in the value of α_g. Typical available literature values of α for semicrystalline PET are $1.7\cdot10^{-4}$ and $3.94\cdot10^{-4}$ K^{-1} below and above T_g, respectively, and for equilibrium melt $6.55\cdot10^{-4}$ K^{-1} [27]. For comparison, the values calculated from *pvT* isobars extracted at ambient pressure presented in [31] are $\alpha_l=dv/dT=6.19\cdot10^{-4}$ cm^3 g^{-1} K^{-1} for equilibrium melt between 270–320°C and $\alpha_g=dv/dT=1.55\cdot10^{-4}$ cm^3 g^{-1} K^{-1} below T_g (22–64°C) for PET crystallized during cooling from melt, leading to some $\alpha_g=2.2\cdot10^{-4}$ K^{-1} using appropriate specific volume. Data comparable with α_l in the present context can be found in [32]; it was obtained with the help of a mercury dilatometer in the temperature range of 80–100°C. For amorphous PET, value $\alpha_l=4.5\cdot10^{-4}$ cm^3 g^{-1} K^{-1} was determined, leading to $\alpha_l=6.16\cdot10^{-4}$ K^{-1} for ν=0.7296 cm^3 g^{-1} measured at T=84.7°C [31]. As can be seen, the values published earlier are comparable with our results.

In general, it was proved by experimental results that the presence of crystals affects the thermal properties of semicrystalline PET. The difference in thermal expansion coefficient associated with glass transition as an attribute of the amorphous phase does not decrease in direct proportion with crystallinity. The data shows a strong deviation from two-phase system linear trend. Further, the missing amount of $\Delta\alpha$ indicates the presence of the rigid amorphous fraction. This can be calculated incorporating a three-phase model when amorphous and crystalline fractions are smaller than unity. In case of a three-component system containing two amorphous regions, RAF and MAF, together with the crystalline region (with the

assumption of their volumes additive), the total volume, V, can be given as

$$V = V_c + V_{MAF} + V_{RAF} \quad (6)$$

where V_c, V_{MAF} and V_{RAF} are the volumes of the corresponding phases. Then the volume fraction of the i^{th} element is defined as

$$\varphi_{(i)} = \frac{V_{(i)}}{\sum_i V_{(i)}} \quad (7)$$

leading to:

$$1 = \varphi_c + \varphi_{MAF} + \varphi_{RAF} \quad (8)$$

The volume changes in glass transition transformation (vitrification), represented here by the value of $\Delta\alpha$, are considered to be a contribution of the transformation of MAF from melt to the glassy state. The temperature dependence of V_{RAF} or V_c is not supposed to have sudden changes in T_g region, so their values do not contribute to the jump in α at T_g. Using this assumption, the volume fraction of MAF can be estimated from relation

$$\varphi_{MAF} \approx \frac{\alpha_l - \alpha_g}{\alpha_{l,a} - \alpha_{g,a}} = \frac{\Delta\alpha}{\Delta\alpha_a} \quad (9)$$

where, $\Delta\alpha_a$ represents the difference in thermal expansion coefficients in the glass transition region for completely amorphous PET and $\Delta\alpha$ for its semicrystalline modification.

The mobile amorphous fraction, φ_{MAF}, decreases with crystalline content, φ_c, as can be seen in Table 1 (and also in Fig. 4). The quantity φ_{RAF}, on the other hand, gradually increases with φ_c up to 20.9 vol.%, then it slightly decreases at pseudo-equilibrium. The achieved values of RAF in the present paper, around 44 vol.%, are very similar to the literature data measured for cold-crystallized PET; despite the fact that all available literature data represents mass fraction of RAF, as they are usually achieved by calorimetric measurements. For example, for cold-crystallized PET with the crystallinity of about 24–27% the portion of RAF is between 37 and 49% [3, 5, 30]. On the other hand, melt-crystallized PET presents much lower content of RAF, e.g. for recrystallization temperature 210°C, where the crystallinity reaches 35%, the content of RAF is only 14% [5], compared to our present research, where at 245°C recrystallization the crystallinity is as high as 50 vol.% but the portion of RAF only 4%, which is an extremely low value.

The values of specific RAF defined as the average of the fraction of rigid amorphous structure per crystal, φ_{RAF}/φ_c, were also calculated. As can be seen from Fig. 4 (and Table 1), the values are reduced during cold-crystallization from 5.4 for the original PET to 1.7

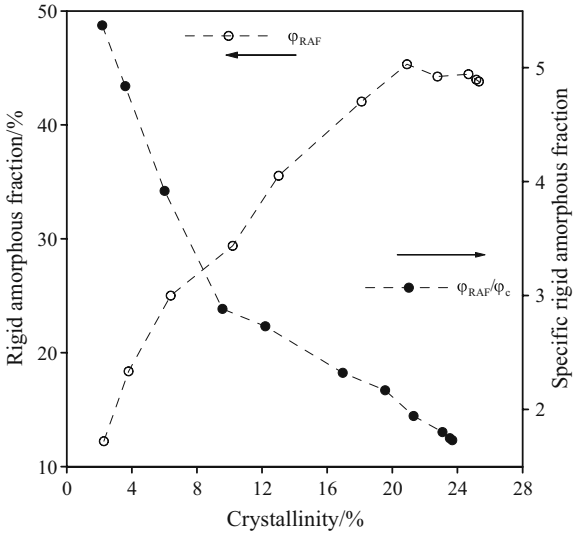

Fig. 4 Dependences of rigid amorphous fraction and specific rigid amorphous fraction on crystallinity content for cold-crystallized PET at 106°C

at pseudo-equilibrium, and further by subsequent annealing. For highly crystallized PET the fraction of RAF per crystal achieves a very low value (0.1). The described decrease in the amount of RAF, as a result of longer cold-crystallization at 106°C, but mainly after re-crystallization at 245°C, can be attributed to crystal perfection when the strain transmitted to the amorphous phase is reduced. A similar effect was observed in a calorimetric study [3], where specific RAF also decreased from values >5 to some 1.7–1.8 at the crystallinity of 24% after finished cold-crystallization and finally decreased to about 0.7–0.8 after annealing at 240°C reaching crystallinity 44%.

Conclusions

The research has shown that the two-phase model is not able to describe the structure of semicrystalline PET. The difference in thermal expansion coefficients, $\Delta\alpha$ associated with T_g does not change in direct proportion with crystallinity. Instead, a missing amount of $\Delta\alpha$ was found, which proves the presence of the rigid amorphous fraction, RAF. Incorporating a three-phase model, the amount of RAF was estimated and found to increase with crystallinity; its maximum value is ca. 45 vol.% at pseudo-equilibrium for cold-crystallized PET. On the other hand, the proportion of RAF per crystal continuously decreases. Such changes can be explained by progressing crystallization process in the material, connected with the construction of more complex crystalline structure and crystal perfection. Further high temperature annealing causing PET recrystallization leads to a dramatic reduction of the RAF content.

As the RAF portion affects processing characteristics or content of acetaldehyde in recycled PET, its content is an important factor in the material manufacture in practice.

Acknowledgements

The financial support of the Ministry of Education, Youth and Sports of the Czech Republic in the frame of project MSM7088352101 is gratefully acknowledged.

References

1 B. Wunderlich, Prog. Polym. Sci., 28 (2003) 383.
2 B. Wunderlich, Macromol. Rapid Commun., 26 (2005) 1521.
3 R. Androsch and B. Wunderlich, Polymer, 46 (2005) 12556.
4 M. Song, J. Appl. Polym. Sci., 81 (2001) 2779.
5 J. Lin, S. Shenogin and S. Nazarenko, Polymer, 43 (2002) 4733.
6 M. Song and D. J. Hourston, J. Therm. Anal. Cal., 54 (1998) 651.
7 R. Rastogi, P. Vellinga, S. Rastogi, C. Schick and H. E. H. Meijer, J. Polym. Sci. Pol. Phys., 42 (2004) 2092.
8 J. Hadač, P. Slobodian and P. Sáha, J. Mater. Sci., DOI 10. 1007/s10853-006-0378-z (2007).
9 J. D. Menczel and M. Jaffe, J. Therm. Anal. Cal., 89 (2007) 357.
10 N. M. Alves, J. F. Mano, E. Balaguer, J. M. Meseguer Dueñas and J. L. Gómez Ribelles, Polymer, 43 (2002) 4111.
11 S. Montserrat and P. Cortés, J. Mater. Sci., 30 (1995) 1790.
12 G. Vigier and J. Tatibouet, Polymer, 34 (1993) 4257.
13 A. Aref-Azar, F. Arnoux, F. Biddlestone and J. N. Hay, Thermochim. Acta, 273 (1996) 217.
14 W. Dong, J. Zhao, Ch. Li, M. Guo, D. Zhao and Q. Fan, Polym. Bull., 49 (2002) 197.
15 G. Vigier, J. Tatibouet, A. Benatmane and R. Vassoille, Colloid Polym. Sci., 270 (1992) 1182.
16 K. Fukao and Y. Miyamoto, J. Non-Cryst. Solids, 211 (1997) 208.
17 B. G. Olson, J. Lin, S. Nazarenko and M. Jamieson, Macromolecules, 36 (2003) 7618.
18 G. Dlubek, A. S. Gupta, J. Pionteck, R. Hassler, R. Krause-Rehberg, H. Kaspar and K. H. Lochhaas, Polymer, 46 (2005) 6075.
19 H. Chen and P. Cebe, J. Therm. Anal. Cal., 89 (2007) 417.
20 C. Schick, A. Wurm, M. Merzlyakov, A. Minakov and H. Marand, J. Therm. Anal. Cal., 64 (2001) 549.
21 R. K. Krishnaswamy, J. F. Geibel and B. J. Lewis, Macromolecules, 36 (2003) 2907.
22 Y. M. Wang, S. S. Funari and J. F. Mano, Macromol. Chem. Phys., 207 (2003) 11262.
23 C. Schick, J. Dobbertin, M. Potter, H. Dehne, A. Hensel, A. Wurm, A. M. Ghoneim and S. Weyer, J. Thermal Anal., 49 (1997) 499.
24 L. C. E. Struik, Polymer, 28 (1987) 1534.
25 Y. G. Fu, B. Annis, A. Boller, Y. M. Jin and B. Wunderlich, J. Polym. Sci. Pol. Phys., 32 (1994) 2289.
26 ASTM Standard D 864-52 (1952).
27 J. Brandrup and E. H. Immegut, Polymer Handbook the 3rd Ed., Wiley & Sons Inc., New York 1989, p. V/101.
28 S. Fakirov, E. V. Fischer and G. F. Schmidt, Macromol. Chem., 176 (1975) 2459.
29 R. M. R. Wellen and M. S. Rabello, J. Mater. Sci., 40 (2005) 6099.
30 C. Schick, L. Krämer and W. Mischok, Acta Polym., 36 (1985) 47.
31 P. Zoller and D. Walsh, Standard Pressure-Volume-Temperature Data for Polymers, Technomic Publishing Co. Inc., Lancaster 1995, p. 323.
32 K. H. Hellwege, J. Hennig and W. Knappe, Kolloid-zeitschrift and Zeitschrift für Polymere, 186 (1962) 29.

Received: May 9, 2007
Accepted: April 23, 2008
OnlineFirst: August 15, 2008

DOI: 10.1007/s10973-007-8566-x